Overview on Performance Lower Bounds for Blind Frequency Offset Estimation

N. Noels, P. Ciblat, and H. Steendam

***Abstract*—This paper focusses on performance bounds for estimating the frequency and the phase of a received signal, when the complex amplitude of the signal is non-constant and unknown. In many application fields receivers need to perform such an estimation: digital communications, direction of arrival estimation, Doppler radar, etc... While in digital communications the non-constant complex signal amplitude is a discrete random variable related to the transmitted information bits, in many other signal processing fields this non-constant amplitude is typically modelled as multiplicative Gaussian noise. Fundamental lower bounds on the mean square error of any frequency offset and phase shift estimator are continuously employed in all these application fields. They serve as a useful benchmark to judge the performance of practical estimators. We present an overview of such bounds with their respective interests and their associated derivations in closed-form.**

I. Introduction and Motivation

Let us consider digital bandpass communication over an additive white Gaussian noise (AWGN) channel using linear modulation. An information bit sequence is first channel encoded and then mapped to a block of complex numbers (data symbols) belonging to a discrete symbol constellation set Ω. The *channel encoder* introduces structured redundancy in the transmitted bit sequences; this makes it possible to detect and correct some of the occurred bit errors at the receiver. *Symbol mapping* is performed to improve the bandwidth efficiency. The resulting data symbols are first applied to a square-root Nyquist transmit filter and then multiplied to a sinusoidal transmit carrier signal in order to obtain a signal that is suitable for transmission over the bandpass channel. At the receiver end, the received signal is multiplied with a carrier signal matched to the transmit carrier signal, applied to a filter matched to the transmit filter and sampled at the correct time instants.

To enable a reliable detection of the transmitted information bits from the resulting observation samples, it is imperative that the carrier signals at the transmitter and the receiver have almost exactly the same frequency and phase. However, as the carrier oscillators at the transmitter and receiver are operating independently, their frequency and phase are not the same, and the demodulation at the receiver is performed using a local reference carrier signal that exhibits a frequency offset φ_1 and a phase shift $2\pi\varphi_0$ vis-à-vis the received modulated carrier signal. In that case, the observation samples can be modelled as a noisy version of a complex sinusoid with frequency φ_1 and phase $2\pi\varphi_0$ and with a non-constant complex-valued amplitude equal to the unknown transmitted data symbols or realizations of a multiplicative Gaussian noise process. In order to cope with the unknown parameters φ_0 and φ_1 the receiver is fitted with an estimation unit which has to estimate the quantities φ_0 and φ_1 from the observation samples. Once the frequency offset and the phase shift have been estimated, the demodulated signal is *corrected* in order to compensate for them. The detection unit of the receiver subsequently decides upon the received information bits based on the corrected observation samples, assuming perfect frequency offset and phase shift compensation. A result of the latter assumption is that the accuracy of the estimation unit has direct repercussions on the accuracy of the detection unit.

Besides from a mismatch between transmit and receive carrier frequency, the frequency offset φ_1 can also result from the so-called Doppler effect. If a vehicle is transmitting information to the receiver side and is simultaneously moving, the transmit carrier frequency is modified by the Doppler effect and the receiver is not well adapted in frequency. This Doppler effect, which is a drawback in digital communications, can be of great interest in some applications. For instance, radar based on Doppler effect is able to find the velocity of a target. In other applications, such as Direction-of-Arrival (DOA) estimation, the spatial frequency related to angle-of-arrival in an array processing can be mathematically seen as a carrier frequency offset. As a consequence, besides digital communications, there are a lot of applications for which it is needed to estimate a frequency disturbed by a non-constant amplitude. Unlike digital communications, this non-constant amplitude is not associated with information bits but with other parameters such as the Doppler spread for Doppler radar or the spatial distribution of the source for DOA estimation [1]–[3].

Estimation accuracy is usually measured by the mean square estimation error (MSEE). This is the expected value of the squared difference between the estimated and the true value of the frequency offset and the phase shift. The estimation unit which minimizes the MSEE is referred to as the *minimum mean square error* (MMSE) estimator. In many practical situations MMSE estimation gives rise to a prohibitive computational burden and one has to resort to approximation techniques. The various existing estimation units are the result of applying these techniques (see, e.g., [4]).

Rapid developments in digital communications [5]–[8] and signal processing applications [1]–[3] cause a nonstop increase of the requirements that are imposed on the estimation units' design. This also provides a constant impulse to the research on fundamental lower bounds on the attainable estimation accuracy (see, e.g., [1]–[3], [9]–[20], [20]–[31]). On the one hand, such bounds serve as a useful benchmark to judge the performance of practical estimators. On the other hand, if interpretable closed-form expressions exist, they also might provide useful insight into the influence of the various signal parameters on the achievable estimation accuracy.

In this tutorial, we focus on the derivation and the analysis of such bounds. One of the most celebrated performance limits is the Cramer-Rao bound (CRB) [32], which is known to be a tight bound for a wide class of estimators, provided that the SNR is sufficiently high. In the considered applications, the statistics of the observation samples depend not only on the frequency offset and the phase shift to be estimated but also on the statistics of the non-constant amplitude. This makes the computation of the CRB far from trivial. In order to avoid the computational complexity associated with the true CRB several alternative Cramer-Rao-like bounds have also been proposed in the literature (see, e.g., [2], [9], [10], [14], [26], [31]). We present an overview of these bounds with their respective interests and their associated derivations in closed-form for various cases (coded/non-coded digital modulation, circular/non-circular multiplicative noise). It is well-known that the CRB (and in particular the CRB for frequency offset estimation) is not accurate at low SNR and/or when the number of observation samples becomes too small [33]. The large gap between the CRB and the MSEE of practical frequency offset estimators is the result of the estimators sporadically making large errors referred to as outliers. To analyze this phenomenon, we also discuss the Barankin bound (BB) [27]–[29] and the Ziv-Zakai bound (ZZB) [20] for frequency offset estimation which are more complicated bounds to compute but which are considerably tighter than the CRB at low SNR.

II. Problem Formulation

Throughout the paper, the following signal model is considered:

$$r(n) = a(n)e^{2\pi j(\varphi_0+\varphi_1 n)} + w(n), \tag{1}$$

for $n = k_0, ..., k_0 + N - 1$, where

- $a(n)$ is a priori unknown and is referred to as either "multiplicative noise" or "non-constant amplitude".
- φ_0 and φ_1 are the normalized phase shift (at n=0) and the normalized frequency offset of the received signal. These parameters are also a priori unknown to the receiver and need to be estimated. The absolute value of k_0 determines the difference (in number of symbol intervals) between the start of the received signal and the time instant at which the phase shift φ_0 is estimated.
- $w(n)$ is circularly-symmetric complex-valued AWGN with zero-mean and variance σ_w^2.

By stacking all the available observations into a row vector, we have

$$\mathbf{r} = \mathbf{a}\mathbf{S}\left([\varphi_0, \varphi_1]\right) + \mathbf{w}, \tag{2}$$

where

- $\mathbf{w}$ is a Gaussian noise vector with zero mean, $\mathbb{E}\left[\mathbf{w}^{\mathrm{T}}\mathbf{w}\right] = \mathbf{0}_N$, and $\mathbb{E}\left[\mathbf{w}^{\mathrm{H}}\mathbf{w}\right] = \sigma_w^2\mathbf{I}_N$, where $\mathbf{0}_k$ represents a $k \times k$ null matrix and $\mathbf{I}_k$ represents a $k \times k$ identity matrix. The superscripts $(.)^{\mathrm{T}}$ and $(.)^{\mathrm{H}}$ stand for the transposition and the conjugate-transposition operators respectively.
- $\mathbf{S}\left([\varphi_0, \varphi_1]\right)$ is a diagonal matrix with the n-th diagonal element given by

$$S\left(n, n; [\varphi_0, \varphi_1]\right) = e^{2\pi j(\varphi_0+\varphi_1 n)},$$

such that $\mathbf{S}\left([\varphi_0, \varphi_1]\right)\mathbf{S}^{\mathrm{H}}\left([\varphi_0, \varphi_1]\right) = \mathbf{I}_N$.

The signal model (1)-(2) is encountered in several application fields. A first example is that of digital bandpass communication over an AWGN channel using linear modulation. In that case, $a(n)$ represents the nth data symbol passing through the digital bandpass communication channel. The data symbols result from an information bit sequence which is first channel encoded (for better bit error protection) and then mapped (for higher bandwidth utilization) to a block of complex numbers belonging to a discrete set Ω, referred to as the symbol constellation. In the digital communications case, we will also consider that $\sigma_w^2 = N_0/E_s$, with N_0 and E_s assumed to be known. Here, N_0 denotes the noise power spectral density and E_s is the symbol energy. The ratio E_s/N_0 is an important measure for the signal quality at the receiver and is commonly referred to as the *signal-to-noise ratio* (SNR).

As already evoked, other application fields where the signal model (1) can be encountered are that of DOA estimation and Doppler radar. In DOA estimation, $a(n)$ represents the spatial distribution of the source. In Doppler radar, $a(n)$ represents the Doppler spread of the reference signal. In both cases, it is standard to model the non-constant amplitude as a Gaussian process [1], [3], [34]. Even in digital communications, the process $a(n)$ can be sometimes viewed a Gaussian one: indeed, in a flat fading channel, $a(n)$ can be the product between a transmitted symbol and a non-constant complex amplitude related to the channel quality. In a Non-Line-of-Sight (NLOS) channel, due to the various scatterers, it is usual to consider that non-constant amplitude as a Gaussian process and so its magnitude as a Rayleigh process. Therefore it is also referred to as the so-called Rayleigh channel, e.g., [35].

For the sake of completeness, we note that (1) is only approximate and in particular valid only when $|\varphi_1| << 1$ [15].

From the observation samples $\{r(n)\}$ (1), we now want to recover the value of a deterministic parameter vector $\mathbf{u}$ with components u_0, u_1, ... This vector contains (but is not restricted to) the unknown phase shift φ_0 and frequency offset φ_1. A common approach to evaluate the quality of an unbiased estimator for $\mathbf{u}$ consists in comparing its resulting MSEE with a CRB or some other tight fundamental lower bound on the achievable MSEE.

III. Deriving the CRB

The CRB results from the inequality $\mathbf{R}_{\mathbf{u}} - \mathbf{J}^{-1} \geq \mathbf{0}$ [32]. Here, $\mathbf{R}_{\mathbf{u}}$ is the error correlation matrix related to the estimation of a deterministic parameter vector $\mathbf{u}$, the notation $\mathbf{A} \geq \mathbf{0}$ indicates that $\mathbf{A}$ is a positive semi-definite matrix, and $\mathbf{J}^{-1}$ denotes the inverse of the Fisher Information Matrix (FIM) $\mathbf{J}$. The elements of $\mathbf{J}$ are given by

$$J_{u_k,u_l} = \mathbb{E}\left[\ell_k\left(\mathbf{u};\mathbf{r}\right)\ell_l\left(\mathbf{u};\mathbf{r}\right)\right], \tag{3}$$

where J_{u_k,u_l} corresponds to the joint Fisher information for the parameters (u_k, u_l), where $\mathbb{E}[.]$ denotes averaging with respect to $p\left(\mathbf{r}|\mathbf{u}\right)$, and where

$$\ell_k\left(\mathbf{u};\mathbf{r}\right) = \frac{\partial \ln p\left(\mathbf{r}\,|\mathbf{u}\right)}{\partial u_k}$$

is a short-hand notation for the derivative of $\ln p(\mathbf{r}|\mathbf{u})$ with respect to the k-th parameter u_k of $\mathbf{u}$. It easily follows from $\mathbf{R_u} - \mathbf{J}^{-1} \geq \mathbf{0}$ that

$$\mathbb{E}\left[(u_k - \hat{u}_k)^2\right] \geq \text{CRB}(u_k), \tag{4}$$

where $\text{CRB}(u_k)$ is the k-th diagonal element of the inverse of the FIM $\mathbf{J}$. The right-hand side of the above expression is referred to as the CRB.

A. Non-constant complex amplitude = digital data symbol

In this section we derive the exact CRB, or equivalently the exact FIM, for the deterministic parameter vector $\mathbf{u} = [u_0, u_1] = [\varphi_0, \varphi_1]$ from N samples of a received linearly modulated digital communication signal in AWGN. We recall that we consider the signal model given by (1)-(2). As usually done in digital communications, we model the symbol vector $\mathbf{a}$ as a discrete random vector with the following uniform a priori distribution:

$$\Pr[\mathbf{a} = \tilde{\mathbf{a}}] = \begin{cases} 2^{-N_b} & , \tilde{\mathbf{a}} \in \mathcal{S}_0 \\ 0 & , \tilde{\mathbf{a}} \in \mathcal{S} \backslash \mathcal{S}_0 \end{cases}. \tag{5}$$

Here, $\mathcal{S}$ denotes the set of all possible vectors of N symbols taking values in the symbol constellation set Ω, and $\mathcal{S}_0 \subset \mathcal{S}$ denotes the subset of these vectors that result from encoding and mapping an information bit sequence. The distribution (5) reflects that a one-to-one correspondence exists between the set of all possible sequences of N_b information bits and the data symbol vectors in S_0, while the receiver has no prior knowledge about the transmitted information bit sequence. It is further standard to assume that $\mathbb{E}[\mathbf{a}] = 0$ and that $\mathbb{E}\left[\mathbf{a}^{\text{H}}\mathbf{a}\right] = \mathbf{I}_N$. This assumption holds true for transmissions without channel encoding and is approximately valid for most practical coded modulation schemes [36].

A brute force numerical evaluation of the FIM related to the estimation of $\mathbf{u}$ involves replacing in (3) the statistical average $\mathbb{E}[.]$ by an arithmetical average over a large number of realizations of $\mathbf{r}$, that are computer-generated according to the conditional distribution $p(\mathbf{r}|\mathbf{u})$. The numerical evaluation of the FIM further requires the computation of the derivatives $\ell_k(\mathbf{u};\mathbf{r})$, $k = 0, 1$ that correspond to the realizations of $\mathbf{r}$ given $\mathbf{u}$. These derivatives can be put into the following form [37]:

$$\ell_k(\mathbf{u};\mathbf{r}) = \sum_{\tilde{\mathbf{a}}} \frac{\partial \ln p(\mathbf{r}|\mathbf{a} = \tilde{\mathbf{a}}, \mathbf{u})}{\partial u_k} \Pr[\mathbf{a} = \tilde{\mathbf{a}}|\mathbf{r}, \mathbf{u}], \tag{6}$$

As $p(\mathbf{r}|\mathbf{a}, \mathbf{u})$ is Gaussian, the logarithm $\ln p(\mathbf{r}|\mathbf{a}, \mathbf{u})$ is readily available in closed-form:

$$\ln p(\mathbf{r}|\mathbf{a}, \mathbf{u}) \propto -\frac{E_s}{N_0} |\mathbf{r} - \mathbf{a}\mathbf{S}(\mathbf{u})|^2.$$

Differentiating with respect to u_k yields

$$\frac{\partial \ln p(\mathbf{r}|\mathbf{a}, \mathbf{u})}{\partial u_k} = -\frac{2E_s}{N_0} \Re\left\{ (\mathbf{r} - \mathbf{a}\mathbf{S}(\mathbf{u}))^{\text{H}} \left(\mathbf{a} \frac{\partial \mathbf{S}(\mathbf{u})}{\partial u_k} \right) \right\}.$$

The joint symbol a posteriori probabilities (APP) $\Pr[\mathbf{a}|\mathbf{r}, \mathbf{u}]$ in (6) can be computed from $p(\mathbf{r}|\mathbf{a}, \mathbf{u})$ and $\Pr[\mathbf{a}]$, according to

$$\Pr[\mathbf{a}|\mathbf{r}, \mathbf{u}] = \frac{\Pr[\mathbf{a}] p(\mathbf{r}|\mathbf{a}, \mathbf{u})}{\sum_{\tilde{\mathbf{a}}} p(\mathbf{r}|\mathbf{a} = \tilde{\mathbf{a}}, \mathbf{u}) \Pr[\mathbf{a} = \tilde{\mathbf{a}}]}. \tag{7}$$

Although this procedure yields the exact derivatives $\ell_k(\mathbf{u};\mathbf{r})$, $k = 0, 1$, the summations in (6) and (7) gives rise to a computational complexity that is exponential in the burst size N.

It is shown in [16], [37] that the computational complexity associated with the evaluation of the CRB can be drastically reduced by taking into account the specific (linearly modulated) structure of the useful signal in (1).

Because $\mathbf{S}(\mathbf{u})\mathbf{S}^{\text{H}}(\mathbf{u}) = \mathbf{I}_N$ does not depend on $\mathbf{u}$, we obtain

$$\frac{\partial \ln p(\mathbf{r}|\mathbf{a}, \mathbf{u})}{\partial u_k} = \frac{2E_s}{N_0} \Re\left\{ \mathbf{r} \left(\frac{\partial \mathbf{S}(\mathbf{u})}{\partial u_k} \right)^{\text{H}} \mathbf{a}^{\text{H}} \right\}.$$

Substituting the above expression into (6), then yields

$$\ell_k(\mathbf{u};\mathbf{r}) = \frac{2E_s}{N_0} \Re\left\{ \mathbf{r} \left(\frac{\partial \mathbf{S}(\mathbf{u})}{\partial u_k} \right)^{\text{H}} \boldsymbol{\mu}^{\text{H}}(\mathbf{r}, \mathbf{u}) \right\}, \tag{8}$$

where $\boldsymbol{\mu}(\mathbf{r}, \mathbf{u})$ is a short-hand notation for the a posteriori average of the symbol vector $\mathbf{a}$, with N components

$$\mu(n;\mathbf{r},\mathbf{u}) = \mathbb{E}_{\mathbf{a}}[a(n)|\mathbf{r},\mathbf{u}] \tag{9}$$

$$= \sum_{\omega \in \Omega} \omega \Pr[a(n) = \omega|\mathbf{r},\mathbf{u}], \tag{10}$$

where Ω denotes the set of constellation points and the averaging $\mathbb{E}_{\mathbf{a}}[.|\mathbf{r},\mathbf{u}]$ is with respect to $\Pr[\mathbf{a}|\mathbf{r},\mathbf{u}]$. We emphasize that no approximation is involved in obtaining (10); the right hand side simply expresses the a posteriori average of the n-th data symbol $a(n)$ in terms of the *marginal* APP of $a(n)$, rather than the *joint* APP of all components of $\mathbf{a}$.

Computing the marginal APPs from the joint APP still requires a complexity that increases exponentially with N. However, in most practical scenarios, the required marginal symbol APPs can be directly computed in an efficient way, by applying the sum-product algorithm to a factor graph (FG) representing a suitable factorization of the joint symbol APP [38]. The application of the sum-product algorithm on a graph that corresponds to a tree (i.e., cycle-free FG) is straightforward and yields the exact marginals. When the graph contains cycles, the sum-product algorithm becomes an iterative procedure that, after convergence, yields only an approximation of the marginals. However, when the cycles in the graph are large, the resulting marginals turn out to be quite accurate. When using this FG-based approximation technique to compute the required marginal symbol APPs, computing the derivatives $\ell_k(\mathbf{u};\mathbf{r})$, $k = 0, 1$ according to (8), for a given realization of $\mathbf{r}$ given $\mathbf{u}$, yields a complexity that is linear (and not exponential) in the number of data symbols N. The above expression and evaluation procedure is the main result for the CRB derivations. It allows a fast evaluation of the CRB and holds for any channel code and

any symbol constellation.

For specific hypotheses about the channel code and the symbol constellation, the complexity associated with evaluating the FIM, or equivalently the CRBs, can be further reduced (see, e.g., [12], [13], [15], [19]). We mention a result from [15] for arbitrarily mapped uncoded linear modulation. In that case, all transmitted data symbols are statistically independent and equiprobable, such that the a priori distribution of $\mathbf{a}$ (5) reduces to:

$$\Pr\left[\mathbf{a}=\tilde{\mathbf{a}}\right]=2^{-N_b},\ \forall\tilde{\mathbf{a}}\in\mathcal{S}. \tag{11}$$

Taking into account (11) it is easily verified from (9)-(10) and (7) that the components of the a posteriori average of the data symbol vector $\mathbf{a}$ reduce to:

$$\mu\left(n;r(n),\mathbf{u}\right) = \frac{\sum_{\omega\in\Omega}\omega e^{\left(\frac{E_s}{N_0}\left(2\Re\left\{r(n)e^{-2\pi j(\varphi_0+\varphi_1 n)}\omega^*\right\}-|\omega|^2\right)\right)}}{\sum_{\omega\in\Omega}e^{\left(\frac{E_s}{N_0}\left(2\Re\left\{r(n)e^{-2\pi j(\varphi_0+\varphi_1 n)}\omega^*\right\}-|\omega|^2\right)\right)}}, \tag{12}$$

which only depend on $\mathbf{r}$ through $r(n)$. Taking this into account it was shown in [15] that, with N odd-valued and $k_0=-\frac{1}{2}(N-1)$ (i.e., φ_0 is the phase shift at the burst center), the CRBs can be written into the following form:

$$\left(\mathrm{CRB}\left(\varphi_0\right)\right)^{-1}=8\pi^2\frac{E_s}{N_0}NR_\Omega\left(\frac{E_s}{N_0}\right), \tag{13}$$

$$\left(\mathrm{CRB}\left(\varphi_1\right)\right)^{-1}=\left(\mathrm{CRB}\left(\varphi_0\right)\right)^{-1}\cdot\frac{\left(N^2-1\right)}{12}, \tag{14}$$

where

$$R_\Omega\left(\frac{E_s}{N_0}\right) = \frac{2E_s}{N_0}\mathbb{E}\left[\Im\left\{\mu^*\left(n;r\left(n\right),\mathbf{u}\right)r(n)S^*\left(n,n;\mathbf{u}\right)\right\}^2\right] \tag{15}$$

It is further shown in [15] that $J_{\varphi_0,\varphi_1}=J_{\varphi_1,\varphi_0}=0$. This means that the estimation of the phase shift φ_0 at the center of the observation interval is independent of the frequency φ_1 estimation problem. We observe that $\mathrm{CRB}(\varphi_0)$ is inversely proportional to the number of available signal samples N, whereas $\mathrm{CRB}(\varphi_0)$ is inversely proportional to $N(N^2-1)\approx N^3$, where the approximation holds for large N. We further observe that $\mathrm{CRB}(\varphi_0)$ and $\mathrm{CRB}(\varphi_1)$ are proportional to the same factor $R_\Omega\left(\frac{E_s}{N_0}\right)$ that depends on the symbol constellation and on the SNR, but not on the number of available signal samples. The numerical evaluation of the CRBs from (13)-(14) involves replacing in (15) the statistical average $\mathbb{E}\left[.\right]$ by an arithmetical average over a large number of realizations of $r\left(n\right)S^*\left(n,n;\mathbf{u}\right)$. This procedure is significantly less complex than the evaluation of the FIM entries according to (3) and (8)-(10) using the FG-approach because the a posteriori symbol average (12) is available in closed-form and the average that needs to be computed in (15) is with respect to a complex-valued *scalar* rather than a complex-valued vector of size N.

In spite of all the efforts made in the literature with respect to computing the FIM for linear modulation, an explicit analytical closed-form expression for the CRBs still not exists. The main contribution of the research conducted in [12], [13], [15]–[19] lies in the derivation of new procedures that allow a more efficient (hence faster) numerical evaluation of the CRBs. Unfortunately, the expressions that lead to (and/or come as by-products of) these evaluation procedures usually don't bring much insight into the behaviour of the FIM (e.g., as a function of the parameters that describe the coded modulation scheme).

We will see in the simulation section of the paper that

- For a given symbol constellation set, CRBs for coded and uncoded transmission are equal at sufficiently high SNR. At lower SNR, however, the CRB for coded transmission is significantly lower than the CRB for uncoded transmission.
- For a given channel code, the CRBs increase when the minimum Euclidean distance between the constellation points decreases.

To avoid the computational complexity associated with the evaluation of the true CRBs, asymptotic CRBs (ACRBs) have been considered in [14] and [11], for the case of uncoded linear modulation. This has resulted in closed-form analytical expressions of the CRB that only hold for sufficiently low or high SNR. The high-SNR ACRBs are shown to coincide with the Modified CRB (MCRB). This is another lower bound on the MSEE of any unbiased estimator which is simpler to evaluate but looser than the exact (true) CRB. We will come back on the MCRB later in this paper. For the low-SNR ACRBs the following expressions are presented in [14], assuming N odd-valued and $k_0=-\frac{1}{2}(N-1)$:

$$\left(\mathrm{ACRB}\left(\varphi_0\right)\right)^{-1}_{|\text{low SNR}}=8\pi^2\left(\frac{E_s}{N_0}\right)^L N\frac{L^2|f_L|^2}{L!},$$

$$\left(\mathrm{ACRB}\left(\varphi_1\right)\right)^{-1}_{|\text{low SNR}}=\left(\mathrm{ACRB}\left(\varphi_0\right)\right)^{-1}_{|\text{low SNR}}\cdot\frac{\left(N^2-1\right)}{12}, \tag{16}$$

where L is related to the symmetry angle $\frac{2\pi}{L}$ of the constellation and $f_L=\mathbb{E}\left[\left(a\left(k\right)\right)^L\right]$. We observe that at sufficiently low SNR the CRBs are determined by the symmetry angle of the constellation and evolve inversely proportional to the L-th power of the SNR.

B. Non-constant complex amplitude = a Gaussian process

We recall that we consider the signal model given by (1). We just assume, in the rest of this section that $k_0=0$. However, in this section, we add extra assumptions on the non-constant amplitude $a(n)$. As usually done in Doppler radar, DOA estimation or digital communication over a Rayleigh flat fading channel, the non-constant amplitude $a(n)$ is assumed to be a zero-mean Gaussian stationary process with correlation $c_a(\tau)=\mathbb{E}[a(n+\tau)a^*(n)]$ and pseudo-correlation $p_a(\tau)=\mathbb{E}[a(n+\tau)a(n)]$. The spectrum and pseudo spectrum are denoted respectively as follows

$$C_a(e^{2i\pi f})=\sum_{\tau\in\mathbb{Z}}c_a(\tau)e^{-2i\pi f\tau}$$

and

$$P_a(e^{2i\pi f}) = \sum_{\tau\in\mathbb{Z}} p_a(\tau)e^{-2i\pi f\tau}.$$

By construction, one can remark that $P_a(e^{2i\pi f}) = P_a(e^{-2i\pi f})$. Moreover, the entire statistics $\{c_a(\tau), p_a(\tau)\}_{\tau\in\mathbb{Z}}$ of $a(n)$ only depend on a finite number K of real-valued unknown parameters denoted by $\{\alpha_k\}_{k=1,\ldots,K}$. The non-constant amplitude process $a(n)$ can be real-valued or complex-valued. In the case of a complex-valued process, $a(n)$ can further be *circular* (which means the process distribution is insensitive to any rotation and thus means that $\mathbb{E}[a(n)a(n+\tau)] = 0$ for all τ) or *non-circular* (there exists at least one τ_0 such that $\mathbb{E}[a(n)a(n+\tau_0)] \neq 0$). One can notice that a real-valued process is, by definition, non-circular. Based on the CRB, we will see hereafter that the estimation quality can be split into two classes in regard with the circularity/non-circularity property of the process. In contrast, the estimation performance is independent of the nature of the process values (real or complex). To further information non-circularity property, the reader may refer to [15], [39].

In the sequel, we will first derive the FIM when the number of available samples N is finite (i.e., non-asymptotic case). As once again, the obtained expression for the FIM does not provide additional insights, it is of great interest to further simplify the FIM expression by also considering the case for N going to infinity (i.e., asymptotic case). The resulting CRBs are referred to as Gaussian CRBs (GCRB).

1) Non-asymptotic case: We next derive the exact Gaussian CRB, or equivalently the exact Gaussian FIM $\mathbf{J}$, for the deterministic parameter vector $\mathbf{u} = [\varphi_0, \varphi_1, \sigma_w^2, \alpha_1, \ldots, \alpha_K]$ when N samples of $r(n)$ are available. In order to use well-known results on the FIM [40], we work with real-valued processes. We consider $\breve{\mathbf{r}} = [\Re[\mathbf{r}], \Im[\mathbf{r}]]$ which is a multi-variate Gaussian variable with zero-mean and covariance matrix $\breve{\mathbf{C}}_{\mathbf{r}}$.

The FIM for a multi-variate Gaussian observation vector $\breve{\mathbf{r}}$ has a special form. As one can check that $\breve{\mathbf{C}}_{\mathbf{r}}$ is symmetric, formula (5.2.1) in [40] holds and this leads to

$$J_{u_k,u_l} = \frac{1}{2}\mathrm{Tr}\left(\frac{\partial\breve{\mathbf{C}}_{\mathbf{r}}}{\partial u_k}\breve{\mathbf{C}}_{\mathbf{r}}^{-1}\frac{\partial\breve{\mathbf{C}}_{\mathbf{r}}}{\partial u_l}\breve{\mathbf{C}}_{\mathbf{r}}^{-1}\right),$$

where $\mathrm{Tr}(.)$ is the trace operator.

After straightforward algebraic manipulations, we can show that

$$J_{u_k,u_l} = \frac{1}{2}\mathrm{Tr}\left(\frac{\partial\widetilde{\mathbf{C}}_{\mathbf{r}}}{\partial u_k}\widetilde{\mathbf{C}}_{\mathbf{r}}^{-1}\frac{\partial\widetilde{\mathbf{C}}_{\mathbf{r}}}{\partial u_l}\widetilde{\mathbf{C}}_{\mathbf{r}}^{-1}\right),$$

where $\widetilde{\mathbf{C}}_{\mathbf{r}}$ is the covariance matrix of the random vector $\widetilde{\mathbf{r}} = [\mathbf{r}, \mathbf{r}^*]$ and takes the following form

$$\widetilde{\mathbf{C}}_{\mathbf{r}} = \begin{bmatrix} \mathbf{C}_{\mathbf{r}} & \mathbf{P}_{\mathbf{r}} \\ \mathbf{P}_{\mathbf{r}}^* & \mathbf{C}_{\mathbf{r}}^* \end{bmatrix},$$

with $\mathbf{C}_{\mathbf{r}} = \mathbf{E}[\mathbf{r}^{\mathrm{H}}\mathbf{r}]$ and $\mathbf{P}_{\mathbf{r}} = \mathbf{E}[\mathbf{r}^{\mathrm{T}}\mathbf{r}]$.

One can remark that

$$\widetilde{\mathbf{C}}_{\mathbf{r}} = \widetilde{\mathbf{S}}\left(\widetilde{\mathbf{C}}_{\mathbf{a}} + \sigma_w^2\mathbf{I}_{2N}\right)\widetilde{\mathbf{S}}^{\mathrm{H}},$$

where $\widetilde{\mathbf{S}} = [\mathbf{S}([\varphi_0,\varphi_1]), \mathbf{0}_N; \mathbf{0}_N, \mathbf{S}^*([\varphi_0,\varphi_1])]$, and where $\widetilde{\mathbf{C}}_{\mathbf{a}}$ is defined in a similar way as $\widetilde{\mathbf{C}}_{\mathbf{r}}$. As $\widetilde{\mathbf{C}}_{\mathbf{a}}$ does not depend on the phase parameters, we obtain the following expressions for the FIM

$$\begin{aligned}
J_{\alpha_k,\alpha_l} &= \tfrac{1}{2}\mathrm{Tr}\left(\tfrac{\partial\widetilde{\mathbf{C}}_{\mathbf{a}}}{\partial\alpha_k}(\widetilde{\mathbf{C}}_{\mathbf{a}} + \sigma_w^2\mathbf{I}_{2N})^{-1}\right.\\
&\times \left.\tfrac{\partial\widetilde{\mathbf{C}}_{\mathbf{a}}}{\partial\alpha_l}(\widetilde{\mathbf{C}}_{\mathbf{a}} + \sigma_w^2\mathbf{I}_{2N})^{-1}\right)\\
J_{\sigma_w^2,\sigma_w^2} &= \tfrac{1}{2}\mathrm{Tr}\left((\widetilde{\mathbf{C}}_{\mathbf{a}} + \sigma_w^2\mathbf{I}_{2N})^{-2}\right)\\
J_{\alpha_k,\sigma_w^2} &= \tfrac{1}{2}\mathrm{Tr}\left(\tfrac{\partial\widetilde{\mathbf{C}}_{\mathbf{a}}}{\partial a_k}(\widetilde{\mathbf{C}}_{\mathbf{a}} + \sigma_w^2\mathbf{I}_{2N})^{-2}\right)\\
J_{\varphi_k,\varphi_l} &= 2\pi^2\mathrm{Tr}(\mathbf{D}_k(\widetilde{\mathbf{C}}_{\mathbf{a}} + \sigma_w^2\mathbf{I}_{2N})\mathbf{D}_l(\widetilde{\mathbf{C}}_{\mathbf{a}} + \sigma_w^2\mathbf{I}_{2N})^{-1}\\
&+ \mathbf{D}_l(\widetilde{\mathbf{C}}_{\mathbf{a}} + \sigma_w^2\mathbf{I}_{2N})\mathbf{D}_k(\widetilde{\mathbf{C}}_{\mathbf{a}} + \sigma_w^2\mathbf{I}_{2N})^{-1}\\
&- 2\mathbf{D}_k\mathbf{D}_l)\\
J_{\alpha_k,\varphi_k} &= i\pi\mathrm{Tr}\left(\tfrac{\partial\widetilde{\mathbf{R}}_{\mathbf{a}}}{\partial\alpha_k}[(\widetilde{\mathbf{C}}_{\mathbf{a}} + \sigma_w^2\mathbf{I}_{2N})^{-1}\mathbf{D}_k\right.\\
&- \left.\mathbf{D}_k(\widetilde{\mathbf{C}}_{\mathbf{a}} + \sigma_w^2\mathbf{I}_{2N})^{-1}]\right)\\
J_{\sigma_w^2,\varphi_k} &= 0
\end{aligned}$$

where $\mathbf{D}_k = [\mathbf{d}_k, \mathbf{0}_N; \mathbf{0}_N, -\mathbf{d}_k]$, for $k = 0, 1$ with $\mathbf{d}_0 = \mathbf{I}_N$ and $\mathbf{d}_1 = \mathrm{diag}([0, \cdots, N-1])$. The above expressions are given in [31] and partially in [3] when $a(n)$ is circular and complex-valued. When $a(n)$ is circular and complex-valued, the term $J_{\varphi_0,\varphi_0} = 0$ which means that the constant phase is not identifiable when the pseudo-correlation is zero. Consequently only a non-null pseudo-correlation enables us to estimate the constant phase. Apart from this comment about the constant phase, it is difficult to provide more insights with these expressions and to distinguish the difference between the circular case and the non-circular case. Therefore we move now on to the asymptotic case, i.e., for N sufficiently large.

2) Asymptotic case: When N becomes large, we have to treat the circular case and the non-circular case separately. Let us begin with the circular case.

a) Circular case: When the signal $r(n)$ is circular, one can remark that $r(n)$ is stationary due to our signal model given in (1). This enables us to simplify the asymptotic expressions for the FIM by applying Whittle's formula [41].

In [3], the asymptotic expressions for the CRB are given for $C_a(\tau)$ real-valued and positive. The latter assumption has been justified by many other authors [1], [23]–[25]. For instance, if $a(n)$ is associated with the Doppler spread phenomenon, $C_a(\tau)$ often follows the Jakes model [42], [43] and thus $C_a(\tau) = \sigma_a^2 J_0(\Delta\tau)$ where σ_a^2 is the variance of $a(n)$, Δ is the Doppler spread and $J_0(.)$ is the Bessel function of first kind. In such a case, one can prove that the estimates of $[\varphi_0, \varphi_1]$ are decoupled from the other parameters $[\sigma_w^2, \alpha_1, \cdots, \alpha_K]$. As remarked in the previous subsection, the phase φ_0 can not be estimated in the circular case. As a consequence, we can focus on J_{φ_1,φ_1} only. After tedious algebraic manipulations, one can find that

$$\lim_{N\to\infty}\frac{1}{N}J_{\varphi_1,\varphi_1} = \delta$$

with

$$\delta = \int_0^1 \left(\frac{C_a'(e^{2i\pi f})}{C_a(e^{2i\pi f}) + \sigma_w^2}\right)^2 df$$

and where $C_a'(e^{2i\pi f})$ is the derivative function of $C_a(e^{2i\pi f})$ with respect to f. As the CRB is the inverse of the FIM, we have

$$\mathrm{GCRB}(\varphi_1) \approx \frac{1}{\delta N} \quad \text{(circular case)}.$$

We remark that the frequency can be estimated as soon as $\delta \neq 0$, i.e., as soon as the process $a(n)$ does not have a flat spectrum. Thus, we need to have a coloured Gaussian non-constant amplitude process and not a white Gaussian non-constant amplitude process to be able to estimate the frequency if the process is circular. Moreover the CRB is proportional to $1/N$ and so the minimum achievable MSEE decreases quite slowly with respect to the number of available samples.

b) Non-circular case: Unlike [3], here we can not apply Whittle's formula [41] because $r(n)$ is not stationary with respect to its pseudo-correlation. In the sequel, the introduced results are in fact obtained via theorems dealing with the inversion of (large) Toeplitz matrices ([44], [45]).

After simple but tedious calculations, the FIM is found to be in [31]

$$\begin{array}{rcl}
\lim_{N\to\infty} \frac{1}{N} J_{\alpha_k,\alpha_l} & = & \frac{1}{2}\theta_{k,l} \\
\lim_{N\to\infty} \frac{1}{N} J_{\sigma_w^2,\sigma_w^2} & = & \frac{1}{2}\gamma \\
\lim_{N\to\infty} \frac{1}{N} J_{\alpha_k,\sigma_w^2} & = & \frac{1}{2}\beta_k \\
\lim_{N\to\infty} \frac{1}{N} J_{\varphi_0,\varphi_0} & = & 16\pi^2\xi \\
\lim_{N\to\infty} \frac{1}{N^3} J_{\varphi_1,\varphi_1} & = & \frac{16\pi^2}{3}\xi \\
\lim_{N\to\infty} \frac{1}{N^2} J_{\varphi_0,\varphi_1} & = & 8\pi^2\xi \\
\lim_{N\to\infty} \frac{1}{N} J_{\alpha_k,\varphi_0} & = & 4\pi\mu_k \\
\lim_{N\to\infty} \frac{1}{N^2} J_{\alpha_k,\varphi_1} & = & 2\pi\mu_k
\end{array},$$

where

$$\begin{array}{rcl}
\theta_{k,l} & = & \int_0^1 \frac{1}{\mathcal{X}(e^{2i\pi f})^2} \frac{\partial \mathcal{X}(e^{2i\pi f})}{\partial \alpha_k} \frac{\partial \mathcal{X}(e^{2i\pi f})}{\partial \alpha_l} df \\
& + & \int_0^1 \frac{1}{\mathcal{X}(e^{2i\pi f})} \left(\mathcal{Q}_{k,l}^{(P_a)}(e^{2i\pi f}) - \mathcal{Q}_{k,l}^{(C_a+\sigma_w^2)}(e^{2i\pi f}) \right) df \\
\gamma & = & \int_0^1 \frac{1}{\mathcal{X}(e^{2i\pi f})^2} \big((C_a(e^{2i\pi f}) + \sigma_w^2)^2 \\
& + & (\underline{C_a}(e^{2i\pi f}) + \sigma_w^2)^2 + 2\underline{P_a}(e^{2i\pi f}) P_a(e^{2i\pi f}) \big) df \\
\beta_k & = & \int_0^1 \frac{1}{\mathcal{X}(e^{2i\pi f})} \frac{\partial \mathcal{X}(e^{2i\pi f})}{\partial \alpha_k} df \\
\mu_k & = & \Im m[\int_0^1 \frac{P_a(e^{2i\pi f})}{\mathcal{X}(e^{2i\pi f})} \frac{\partial P_a(e^{2i\pi f})}{\partial \alpha_k} df] \\
\xi & = & \int_0^1 \frac{P_a(e^{2i\pi f}) \overline{P_a(e^{2i\pi f})}}{\mathcal{X}(e^{2i\pi f})} df
\end{array},$$

with

$$\begin{array}{rcl}
\underline{\nu}(e^{2i\pi f}) & = & \overline{\nu(e^{-2i\pi f})} \\
\mathcal{Q}_{k,l}^{(\nu)}(e^{2i\pi f}) & = & \frac{\partial \nu(e^{2i\pi f})}{\partial \alpha_k} \frac{\partial \underline{\nu}(e^{2i\pi f})}{\partial \alpha_l} + \frac{\partial \underline{\nu}(e^{2i\pi f})}{\partial \alpha_k} \frac{\partial \nu(e^{2i\pi f})}{\partial \alpha_l} \\
\mathcal{X}(e^{2i\pi f}) & = & (C_a(e^{2i\pi f}) + \sigma_w^2)(\underline{C_a}(e^{2i\pi f}) + \sigma_w^2) \\
& - & P_a(e^{2i\pi f}) \underline{P_a}(e^{2i\pi f}).
\end{array}.$$

Next we study different scenarios. Firstly, we consider the case where the receiver knows $[\sigma_w^2, \alpha_1, \cdots, \alpha_K]$, i.e., the statistics of multiplicative and additive noises. In this case, the GCRBs result from the inverse of the 2×2 FIM

$$\mathbf{J}_{[\varphi_0,\varphi_1]} = \left[\begin{array}{cc} J_{\varphi_0,\varphi_0} & J_{\varphi_0,\varphi_1} \\ J_{\varphi_0,\varphi_1} & J_{\varphi_1,\varphi_1} \end{array} \right].$$

This yields:

$$\text{GCRB}(\varphi_0)_{|\text{noise statistics known}} = \frac{1}{4\pi^2 \xi N}$$

and

$$\text{GCRB}(\varphi_1)_{|\text{noise statistics known}} = \frac{3}{4\pi^2 \xi N^3}.$$

Secondly, in the case when $[\sigma_w^2, \alpha_1, \cdots, \alpha_K]$ are unknown at the receiver, we obtain (see [31])

$$\text{GCRB}(\varphi_0)_{|\text{noise statistics unknown}} = \text{GCRB}(\varphi_0)_{|\text{noise statistics known}} + \frac{m}{16\pi^2 \xi^2 N}$$

and

$$\text{GCRB}(\varphi_1)_{|\text{noise statistics unknown}} = \text{GCRB}(\varphi_1)_{|\text{noise statistics known}}.$$

Here, m is a bounded scalar taking the following form

$$m = \boldsymbol{\mu}^{\mathrm{T}} \left(\boldsymbol{\theta}/2 - \boldsymbol{\mu}\boldsymbol{\mu}^{\mathrm{T}}/\xi - \boldsymbol{\beta}\boldsymbol{\beta}^{\mathrm{T}}/(2\gamma) \right)^{-1} \boldsymbol{\mu},$$

where $\boldsymbol{\theta} = (\theta_{k,l})_{1\leq k,l\leq K}$, $\boldsymbol{\beta} = (\beta_k)_{1\leq k\leq K}$, $\boldsymbol{\mu} = (\mu_k)_{1\leq k\leq K}$.

Using the previous expressions for the asymptotic CRB, we make the following comments :

- The convergence rates for the phase and frequency estimations are $1/N$ and $1/N^3$ respectively regardless of the color of the multiplicative noise. Recall that for circular complex-valued processes, the phase is not identifiable and the frequency is identifiable only if the multiplicative noise is coloured, with a convergence rate of $1/N$. Notice that a real-valued process can be viewed as a specific case of a non-circular complex-valued process where the imaginary part is zero. Consequently, in terms of performance, the main cut-off is not complex/real but circular/non-circular.
- We recall that the CRB associated with the "pure" frequency estimation issue (i.e., only disturbed by a constant amplitude) is proportional to $1/N^3$ [46]. Consequently, thanks to the non-circularity property of the non-constant amplitude, the non-constant amplitude does not lead to a significant loss in performance.
- Surprisingly, the same frequency estimation performance is obtained whether the statistics of $a(n)$ are known or not.
- The frequency estimation performance depends only on ξ, which refers to an information rate provided by the non-circularity. Indeed, the performance improves when ξ increases.
- In the noiseless case, we observe a floor effect (i.e., $\text{CRB}(\varphi_1) \neq 0$ when $\sigma_w^2 = 0$). This effect vanishes if $C_a(e^{2i\pi f})\overline{C_a(e^{-2i\pi f})} = P_a(e^{2i\pi f})\overline{P_a(e^{-2i\pi f})}$. This condition is fulfilled for example when the multiplicative noise is real-valued.

As a conclusion, we remind that the Gaussian CRB is of interest in many applications: Doppler radar, DOA estimation, digital communication over Rayleigh flat fading channels. If the non-constant amplitude is non-Gaussian, the Gaussian CRB is not a lower bound for the estimation problem anymore. Nevertheless it is still of interest since the Gaussian CRB is a lower bound for any second-order-based estimator (well-adapted to, e.g., digital BPSK modulation) [47]. Consequently, it indicates what is the best expected performance if we carry out an estimator based only on mean and correlation.

Actually in the non-Gaussian case, the non-circularity may also play a significant role. For example, if $a(n)$ is assumed to belong to a QAM modulation, $a(n)$ is circular at second order (i.e., $\mathbb{E}[a(n)a(n)] = 0$) but is non-circular at fourth order

($\mathbb{E}[a(n)a(n)a(n)a(n)] \neq 0$). Thanks to this fourth-order non-circularity, we are able to build an estimator for which the MSEE is proportional to $1/N^3$ and not $1/N$ [47], [48]. This is not in contradiction with the previous results since a QAM modulation is not Gaussian and so the high order statistics of $a(n)$ strongly help to improve the estimation performance.

IV. Deriving the modified CRB

To overcome the complexity concern of deriving the true CRB [1] in the non-Gaussian case, it is possible to define other lower CRB-like bounds that are easier to compute but less tight than the true one. The most well-spread is the so-called *Modified* CRB (MCRB) [9], [10]. Once again, we will restrict our analysis to the estimation of $\mathbf{u} = [\varphi_0, \varphi_1]$. Then the elements of the *Modified* FIM (MFIM) are defined as follows

$$\mathcal{J}_{\varphi_k,\varphi_l} = \mathbb{E}_{\mathbf{a}}\left[\frac{\partial \ln p(\mathbf{r}|\mathbf{u},\mathbf{a})}{\partial \varphi_k}\frac{\partial \ln p(\mathbf{r}|\mathbf{u},\mathbf{a})}{\partial \varphi_l}\right].$$

After standard algebraic manipulations, we obtain that

$$\mathcal{J}_{\varphi_k,\varphi_l} = \frac{8\pi^2}{\sigma_w^2}\mathbb{E}_{\mathbf{a}}[\mathbf{a}\mathbf{d}_k\mathbf{d}_l\mathbf{a}^{\mathrm{H}}].$$

For large N, the resulting MCRBs are given in [9], [10]. We have that

$$\mathrm{MCRB}(\varphi_0) \approx \frac{\left((k_0+N-1)^3-(k_0)^3\right)\sigma_w^2}{2\pi^2 c_a(0)N^4}$$

and

$$\mathrm{MCRB}(\varphi_1) \approx \frac{3\sigma_w^2}{2\pi^2 c_a(0)N^3}.$$

We note that in the case of linear modulation it was assumed that $c_a(0) = 1$ such that the above MCRBs, for N large and odd-valued and $k_0 = (N-1)/2$, reduce to the CRBs from (13)-(14) upon the factor $R_\Omega(\sigma_w^{-2})$ from (15). We have the following comments:

- The derivation of the MCRBs is very easy and enables us to obtain simple closed-form expressions.
- These expressions seem to be "too" simple and do not provide a lot of information since the CRB does not depend on the nature of $a(n)$ (circular/non-circular in Gaussian case, channel code and symbol constellation in non-Gaussian case) while we have seen before that this is crucial information (see profound discussion in Gaussian case and ACRB expressions in non-Gaussian case).
- Nevertheless, the MCRB can be sometimes of great interest. Indeed, if $a(n)$ belongs to a finite set of symbol constellation points Ω, the true CRB (for which no explicit expressions are available) is well approximated by the MCRB at high SNR [11].
- An unexpected consequence of the previous remark is the following. Let us consider the MCRB for estimating the frequency offset in the case of digital communication using a BPSK symbol constellation set, i.e., $a(n)$ takes values in the set $\{-1, 1\}$ which implies that $L = 2$ and $f_L = c_a(0) = 1$. We have

$$\mathrm{MCRB}(\varphi_1)_{\mathrm{BPSK}} \approx \frac{3\sigma_w^2}{2\pi^2 N^3}.$$

Due to previous item, there is equivalence between MCRB and ACRB, at high SNR for BPSK, therefore we know that

$$\mathrm{ACRB}(\varphi_1)_{|\text{high SNR,BPSK}} = \frac{3\sigma_w^2}{2\pi^2 N^3}$$

and thanks to (16), we get

$$\mathrm{ACRB}(\varphi_1)_{|\text{low SNR, BPSK}} = \frac{3\sigma_w^4}{4\pi^2 N^3}.$$

Obviously, at low SNR, the true CRB for BPSK starts seriously deviating from the MCRB.
If we inspect the Gaussian CRB for uncorrelated and real-valued Gaussian $a(n)$, we obtain

$$\mathrm{GCRB}(\varphi_1) = \frac{3\left[2\sigma_w^2+\sigma_w^4\right]}{4\pi^2 N^3}.$$

Surprisingly, the GCRB predicts well the performance of a BPSK based non-constant amplitude for both low AND high SNR whereas a BPSK constellation is not Gaussian at all! Consequently, the GCRB is a powerful tool for analyzing the frequency MSEE in BPSK context whereas the MCRB is not (except at high SNR).

V. Deriving the BB

Let us reconsider the signal model given in (1), with $k_0 = 0$ and $a(n)$ a zero-mean Gaussian stationary process with correlation $c_a(\tau)$ and pseudo-correlation $p_a(\tau)$. For the sake of simplicity, we further assume that the noise statistics, i.e., $\{c_a(\tau), p_a(\tau)\}_{\tau\in\mathbb{Z}}$ and σ_w^2, are known at the receiver. This assumption is made in [49] and partially made in [28] for deriving Barankin bounds (BB) because the computational and analytical complexities are too high otherwise. It can also be noted that the CRB for frequency estimation is insensitive to the knowledge of the noise statistics as soon as the number of samples is large enough (see [31] and GCRB discussion above). We thus can expect that the error induced by neglecting the estimation step with respect to the noise statistics will be sufficiently small so that our further conclusions still hold in case of unknown noise statistics.

To well understand the interest of other bounds than the CRB, let us consider the following example. The signal model is the one from (1) with $a(n)$ a real-valued Gaussian process. To estimate the frequency, as $a(n)$ is non-circular (since real-valued), one can use the so-called square-power estimator [47] defined as follows:

$$\hat{\varphi_1} = \arg\max_{\varphi} \underbrace{\left|\frac{1}{N}\sum_{n=0}^{N-1} r(n)^2 e^{-2j\pi(2\varphi)n}\right|^2}_{F(\varphi)}.$$

In Fig. 1, we plot the MSEE of this estimator and the Modified and Gaussian CRB versus the SNR when $N = 100$.

[1] If the process is Gaussian, the Gaussian CRB is the true one and there are no more concerns due to the results introduced in the previous subsection.

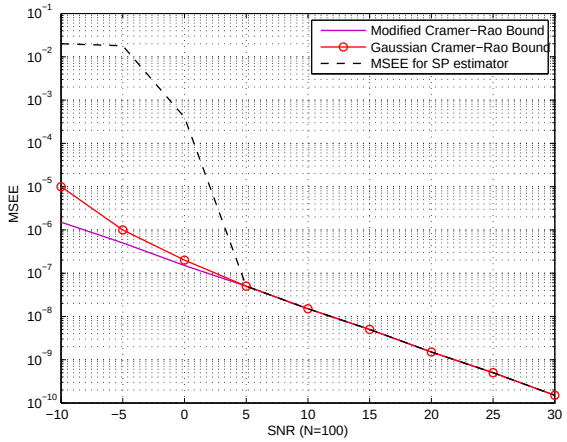

Figure 1. MCRB, GCRB, MSEE for square-power estimator vs. SNR

We observe that at high SNR, the estimator is powerful and even efficient (MSEE equals CRB). In contrast, at low SNR, there is a large mismatch between MSEE and CRB. The question is: is the considered estimator not relevant at low SNR, or, is the CRB not tight enough at low SNR? We will show that the CRB is not tight enough. To demonstrate that, we introduce other lower bounds on the MSEE which are much tighter at low SNR than the CRB.

Now, we can attempt to understand why the CRB is not tight enough at low SNR. In Fig. 2, we plot the cost function $F(.)$ of the square-power estimator for SNR=-5dB (on top) and SNR=5dB (on bottom).

The sought frequency is $\varphi_1 = 0.1$. We remark that, at high SNR, the peak around the true value of the frequency is well detected, whereas, at low SNR, there is a mis-detection of the peak which significantly degrades the performance. Consequently the performance degradation is due to a higher peak far away from the true frequency. These "bad" realizations are called "outliers". By inspecting in detail the FIM from (3), we remark that it depends on the behaviour of the likelihood function around the true frequency since the involved derivative functions are calculated at the true frequency. Therefore the CRB is unable to take into account the mis-detection of the peak and automatically assumes a correct detection of the peak even if it is wrong. Thus at low SNR (when the mis-detection of the peak occurs), the CRB is truly too optimistic.

We are now interested in another bound that inspects the likelihood function around the true frequency but not only there. Therefore we introduce the following set of the so-called "test-points" $\{\boldsymbol{\phi}(k) = [\phi_0(k), \phi_1(k)]^{\mathrm{T}}\}_{1\leq k\leq n}$ at which the likelihood function will be evaluated. We are now able to define the Barankin bound of order p as follows :

$$\mathrm{BB}_p(\varphi_0, \varphi_1) = \sup_{\mathcal{E}} S_p(\mathcal{E})$$

where

$$S_p(\mathcal{E}) = \mathcal{E}(\mathbf{B}(\mathcal{E}) - \mathbf{1}_p\mathbf{1}_p^{\mathrm{T}})^{-1}\mathcal{E}^{\mathrm{T}}$$

with $\mathcal{E} = [\boldsymbol{\phi}(1) - \mathbf{u}^{\mathrm{T}}, \ldots, \boldsymbol{\phi}(p) - \mathbf{u}^{\mathrm{T}}]$, and $\mathbf{1}_p = \mathrm{ones}(p, 1)$.

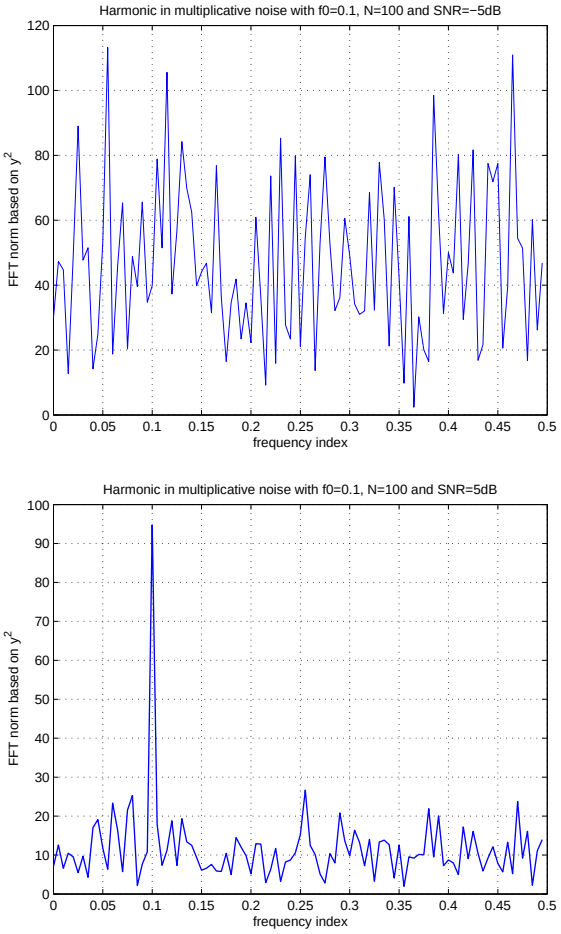

Figure 2. Cost function $F(\varphi)$ vs φ for $\mathrm{SNR} = -5\mathrm{dB}$ (top) and $\mathrm{SNR} = 5\mathrm{dB}$ (bottom)

The term $\sup$ stands for the smallest upper bound on the set $\mathcal{E}$. Furthermore $\mathbf{B}(\mathcal{E}) = (B_{k,l})_{1\leq k,l\leq p}$ is the following $p \times p$ matrix

$$B_{k,l} = \mathbb{E}[L(\mathbf{r}, \mathbf{u}, \boldsymbol{\phi}(k))L(\mathbf{r}, \mathbf{u}, \boldsymbol{\phi}(l))],$$

with

$$L(\mathbf{r}, \mathbf{u}, \boldsymbol{\phi}(k)) = \frac{p(\mathbf{r}|\boldsymbol{\phi}(k))}{p(\mathbf{r}|\mathbf{u})}.$$

The MSEE of any unbiased estimator is greater than the Barankin bound of any order p ([40]). From an asymptotic point of view (as $p \to \infty$), the Barankin bound is even the tightest lower bound that one can find ([27], [28]). As for the choice of the test-points, it is usual to consider the following structure for $\mathcal{E}$ ([28], [29]):

$$\mathcal{E} = \begin{bmatrix} \phi_0 - \varphi_0 & 0 \\ 0 & \phi_1 - \varphi_1 \end{bmatrix} = \mathrm{diag}(\varepsilon_0, \varepsilon_1). \qquad (17)$$

Our main concern hereafter is to derive in closed-form expression the matrix $\mathbf{B}$ for such test-points.

Let us now remind some notations. The covariance matrix $\widetilde{\mathbf{C}}_{\mathbf{r}}(\boldsymbol{\phi})$ of the multivariate process $\widetilde{\mathbf{r}}$ can be written as follows

$$\widetilde{\mathbf{C}}_{\mathbf{r}}(\boldsymbol{\phi}) = \widetilde{\mathbf{S}}(\boldsymbol{\phi})\left(\widetilde{\mathbf{C}}_{\mathbf{a}} + \sigma_w^2\mathbf{I}_{2N}\right)\widetilde{\mathbf{S}}^{\mathrm{H}}(\boldsymbol{\phi}) \qquad (18)$$

where

$$\widetilde{\mathbf{S}}(\boldsymbol{\phi}) = \left[\begin{array}{cc} \mathbf{S}(\boldsymbol{\phi}) & \mathbf{0}_N \\ \mathbf{0}_N & \overline{\mathbf{S}}(\boldsymbol{\phi}) \end{array} \right].$$

After straightforward algebraic manipulations, we finally obtain that

$$B_{k,l} = \left\{ \begin{array}{cc} \frac{1}{\sqrt{\det(\mathbf{Q}_{k,l})}} & \text{if } \mathbf{Q}_{k,l} > 0 \\ +\infty & \text{otherwise} \end{array} \right. ,$$

with

$$\mathbf{Q}_{k,l} = \left(\widetilde{\mathbf{C}}_{\mathbf{r}}(\boldsymbol{\phi}(k))^{-1} + \widetilde{\mathbf{C}}_{\mathbf{r}}(\boldsymbol{\phi}(l))^{-1}\right) \widetilde{\mathbf{C}}_{\mathbf{r}}(\mathbf{u}) - \mathbf{I}_{2N}.$$

These expressions have been introduced in [49] and [28] in a slightly different form (due to the circularity assumption on the non-constant amplitude) and in [31] for the general case.

We now just focus on our main parameter of interest: the frequency φ_1. For the standard test-points described in (17), the Barankin bound for φ_1 takes the following form [28]:

$$\mathrm{BB}(\varphi_1) = \sup_{\varepsilon_0,\varepsilon_1} \frac{\varepsilon_1^2}{(B_{1,1}-1) - \frac{(B_{0,1}-1)^2}{(B_{0,0}-1)}}.$$

The term $(B_{0,1}-1)^2/(B_{0,0}-1)$ represents the loss in performance due to joint phase and frequency parameter estimation.

We remark that the Barankin bound is not strictly speaking obtained in closed-form since the maximum operator still occurs. Nevertheless the existing expressions enable us to compute very fastly the Barankin bound.

As we will see in the simulation part, the Barankin bound enables us to predict partially the outliers effect, i.e, the mismatch between the CRB and the real estimator performance. Consequently the poor estimation performance of the standard square-power estimator (well adapted to BPSK or a real-valued Gaussian process) is shown to be connected to the poor tightness of the CRB. Thus decreasing the gap between the CRB and the estimator performance for a given number of samples at very low SNR is impossible. The CRB is too optimistic in such a context and has to be replaced with the BB.

VI. Deriving the ZZB

To analyze the mismatch between the CRB and the real estimator performance, we have considered the so-called Barankin bound in the previous section. Even though this Barankin bound is much tighter than the CRB and predicts roughly the outliers effect, there is still a mismatch between bound and estimator performance. In this section, we will therefore introduce a third, much more powerful bound, the so-called Ziv-Zakai bound (ZZB).

We note that the ZZB needs a new paradigm on the sought parameters: the so-called Bayesian approach. Unlike previously done, we have to consider the sought parameters as a realization of a random variable. This random variable is further described by a distribution, which characterizes the *a priori* information available on the sought parameters. For instance, for frequency offset estimation, we only know that the frequency is normalized and thus it may take values in the interval $[-1/2, 1/2]$ uniformly.

In [20], [50], it was proved that the following inequality holds for any vector $\mathbf{z} = [z_0, z_1]$

$$\mathbf{z}\mathbf{E}_{\mathbf{u}}\mathbf{z}^{\mathrm{T}} \geq \int_0^{\infty} \Delta \left(\max_{\substack{(\varepsilon_0,\varepsilon_1) \\ z_0\varepsilon_0+z_1\varepsilon_1=\Delta}} f(\varepsilon_0,\varepsilon_1) \right) d\Delta \qquad (19)$$

where $\mathbf{E}_{\mathbf{u}}$ denotes the error correlation matrix related to the estimation of a random variable $\mathbf{u} = [\varphi_0, \varphi_1]$ and

$$f(\varepsilon_0,\varepsilon_1) = \int \min(p(\mathbf{u}), p(\mathbf{u}+\boldsymbol{\varepsilon}))P_e(\mathbf{u}, \mathbf{u}+\boldsymbol{\varepsilon})d\mathbf{u}, \quad (20)$$

with $\boldsymbol{\varepsilon} = [\varepsilon_0, \varepsilon_1]$.

The function $p(\mathbf{u})$ is the *a priori* density function of the bivariate parameter $\mathbf{u}$, and $P_e(\mathbf{u}, \mathbf{u}+\boldsymbol{\varepsilon})$ is the error probability when the optimal detector (namely, the ML detector) is used to decide between the following two hypotheses

$$\left\{ \begin{array}{lrcl} H_0: & y(n) & = & a(n)e^{2i\pi(\varphi_0+\varphi_1 n)} + w(n) \\ H_1: & y(n) & = & a(n)e^{2i\pi((\varphi_0+\varepsilon_0)+(\varphi_1+\varepsilon_1)n)} + w(n) \end{array} \right.$$

where hypotheses H_0 and H_1 are equally likely.

The right hand side of (19) is called the Ziv-Zakai Bound. By inspecting (19), one can remark that the likelihood of $\mathbf{u}$ is scanned over the entire search interval of $\mathbf{u}$, as is also the case for the Barankin bound [31]. Once again, this contrasts with the CRB where the likelihood function is only evaluated around the true point. Therefore we expect that the ZZB can predict the outliers effect at low SNR.

Let us focus now on the ZZB for φ_1, which is obtained by setting $\mathbf{z} = [0, 1]$. Therefore

$$\mathrm{ZZB}(\varphi_1) = \int_0^{\infty} \varepsilon_1 \left(\max_{\varepsilon_0} f(\varepsilon_0,\varepsilon_1) \right) d\varepsilon_1.$$

Actually the MSEE of any (even biaised) estimator for the frequency is greater than the $\mathrm{ZZB}(\varphi_1)$ [20].

The key task now is to express the function $f(.)$ in closed-form. After some simple derivations, one can see that $P_e(\mathbf{u}, \mathbf{u}+\boldsymbol{\varepsilon})$ is independent of $\mathbf{u}$, so that it can be denoted by $P_e(\varepsilon_0, \varepsilon_1)$. As a consequence, we have [50]

$$f(\varepsilon_0,\varepsilon_1) = g(\varepsilon_0,\varepsilon_1)P_e(\varepsilon_0,\varepsilon_1)$$

where

$$g(\varepsilon_0,\varepsilon_1) = \int \min(p(\mathbf{u}), p(\mathbf{u}+\boldsymbol{\varepsilon}))d\mathbf{u}.$$

Since we have no *a priori* information on $\mathbf{u}$, we assume that φ_0 and φ_1 are uniformly distributed over $[0, 1/2]$, i.e., the *a priori* distribution of the parameters of interest $p(\mathbf{u})$ is flat. We consider rather the interval $[0, 1/2]$ than $[-1/2, 1/2]$ because the phase and the frequency can only be estimated modulo $1/2$ when multiplicative noise occurs [50]. Consequently

$$g(\varepsilon_0,\varepsilon_1) = (1/2-\varepsilon_0)(1/2-\varepsilon_1).$$

This leads to

$$\mathrm{ZZB}(\varphi_1) = \int_0^{1/2} (1/2-\varepsilon_1)\varepsilon_1 \max_{\varepsilon_0} \left((1/2-\varepsilon_0)P_e(\varepsilon_0,\varepsilon_1)\right) d\varepsilon_1.$$

The rest of the section deals with the evaluation of $P_e(\varepsilon_0, \varepsilon_1)$. After tedious algebraic derivations that can be found in [53], we have

$$P_e(\varepsilon_0,\varepsilon_1) = \mathrm{Prob}\left(\sum_{n=m}^{2N-1} \lambda_n^{(+)} v_n^2 < \sum_{n=0}^{m-1} \lambda_n^{(-)} v_n^2 \right), \quad (21)$$

where

- $\{v_n\}$ is a real-valued i.i.d. Gaussian random process with zero-mean and unit-variance.
- $-\lambda_n^{(-)}$ for $n = 0, \cdots, m-1$ (with $\lambda_n^{(-)} > 0$) are the m negative eigenvalues, and $\lambda_n^{(+)} \geq 0$ for $n = m, \cdots, 2N-1$ are the positive or null eigenvalues of the $2N \times 2N$ matrix $\mathbf{T}(\boldsymbol{\varepsilon})$ defined as follows

$$\mathbf{T}(\boldsymbol{\varepsilon}) = \left(\breve{\mathbf{C}}_{\mathbf{r}}(\boldsymbol{\varepsilon})^{-1} - \breve{\mathbf{C}}_{\mathbf{r}}(0)^{-1}\right)\breve{\mathbf{C}}_{\mathbf{r}}(0),$$

where $\breve{\mathbf{C}}_{\mathbf{r}}(\boldsymbol{\varepsilon}) = \mathbb{E}[\breve{\mathbf{r}}^{\mathrm{T}}\breve{\mathbf{r}}]$ with $\breve{\mathbf{r}} = [\Re[\mathbf{r}], \Im[\mathbf{r}]]$ and $\mathbf{r}$ the received signal disturbed by phase ε_0 and frequency ε_1.

We now wish to derive a closed-form expression for the following term

$$P_e(\varepsilon_0, \varepsilon_1) = \mathrm{Prob}\left(p_+ < p_-\right) \tag{22}$$

where $p_\pm = \sum_n \lambda_n^{(\pm)} v_n^2$ is a weighted sum of squared independent Gaussian variables. Notice that, by construction, p_+ and p_- are independent.

If $\lambda_n^{(+)} = \lambda^{(+)}$ (resp. $\lambda_n^{(-)} = \lambda^{(-)}$) for all corresponding n, then p_+ (resp. p_-) obeys a χ^2 distribution with $(2N-m)$ (resp. m) degrees of freedom. However, if the weighting coefficients are different, the $p_\pm$'s are not χ^2 distributed anymore. Further, expressing the distribution of $p_\pm$ in closed-form is not tractable. Nevertheless, it can be well approximated by means of the Gamma distribution [51]. We recall that the Gamma distribution, denoted $\mathcal{G}(\aleph, \wp)$, is defined as follows

$$P_{\aleph,\wp}(x) = \frac{x^{\aleph-1}}{\Gamma(\aleph)\wp^{\aleph}} e^{-x/\wp}$$

where $\Gamma(.)$ is the so-called Gamma function.

Hence, the distribution of $p_\pm$ is next approximated by the Gamma distribution whose first and second moments are equal to those of $p_\pm$. We thus obtain

$$p_+ \sim \mathcal{G}(\aleph_+, \wp_+) \quad \text{and} \quad p_- \sim \mathcal{G}(\aleph_-, \wp_-)$$

with

$$\aleph_+ = \frac{1}{2}\frac{(\sum_{n=m}^{2N-1}\lambda_n^{(+)})^2}{\sum_{n=m}^{2N-1}{\lambda_n^{(+)}}^2} \text{ and } \wp_+ = 2\frac{\sum_{n=m}^{2N-1}{\lambda_n^{(+)}}^2}{\sum_{n=m}^{2N-1}\lambda_n^{(+)}},$$

and

$$\aleph_- = \frac{1}{2}\frac{(\sum_{n=0}^{m-1}\lambda_n^{(-)})^2}{\sum_{n=0}^{m-1}{\lambda_n^{(-)}}^2} \text{ and } \wp_- = 2\frac{\sum_{n=0}^{m-1}{\lambda_n^{(-)}}^2}{\sum_{n=0}^{m-1}\lambda_n^{(-)}}.$$

As $p_\pm$ is now assumed Gamma distributed, (22) can be simplified. Indeed, by using the fact that the square root of a Gamma distributed random variable is Nakagami distributed, and by using equation (46) in [52], we have that

$$\begin{aligned} P_e(\varepsilon_0, \varepsilon_1) &= \left(\frac{\wp_+}{\wp_-}\right)^{\aleph_+} \frac{\Gamma(\aleph_+ + \aleph_-)}{\aleph_+\Gamma(\aleph_+)} \\ &\times \ {}_2F_1\left(\aleph_+ + \aleph_-, \aleph_+, \aleph_+ + 1; -\frac{\wp_+}{\wp_-}\right) \end{aligned}$$

where ${}_2F_1(.)$ is the so-called hyper-geometric function.

The above expression for $P_e(\varepsilon_0, \varepsilon_1)$ represents the main available result on the ZZB derivations [53]. Although this expression is not interpretable, its numerical computation will provide interesting results as seen below. Notice also that the obtained expressions for the ZZB are not a bound anymore stricly speaking since we are not able to prove that the approximate expressions are less than the exact (but unavailable) bound. But, by checking the approximation numerically, we have observed that the approximation is very tight.

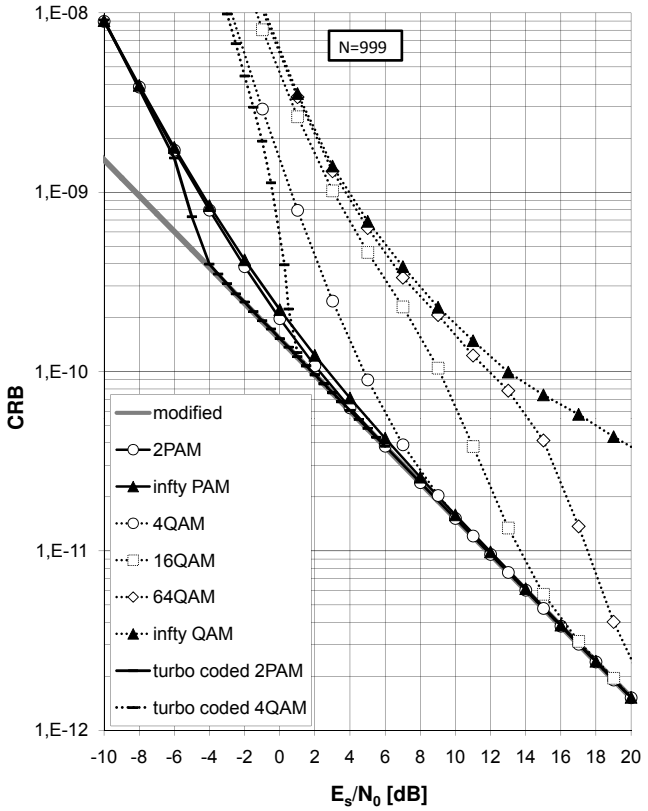

Figure 3. CRBs related to the estimation of φ_1, resulting from the observation model (1) as a function of the SNR E_s/N_0 for random, linear, MPAM and MQAM, coded and uncoded, modulation

VII. Simulation Results

A. Non-constant complex amplitude = digital data symbol

Fig. 3 presents some numerical results for the true CRB regarding the estimation of the frequency offset from the observation of $N = 999$ linearly modulated signal samples that were obtained by means of computer simulations. The following signalling constellations Ω are considered:

- M-ary *Pulse Amplitude Modulation* (M-PAM) for which

$$\Omega = \sqrt{\frac{3}{(M^2-1)}}\mathcal{I}_M.$$

- M-ary *Quadrature Amplitude Modulation* (M-QAM) for which

$$\Omega = \left\{\omega : \Re\{\omega\}, \Im\{\omega\} \in \sqrt{\frac{3}{2(M-1)}}\mathcal{I}_{\sqrt{M}}\right\},$$

where $\Re\{.\}$ and $\Im\{.\}$ denote the real and the imaginary part of a complex number.

In the above,

$$\mathcal{I}_m = \{\pm 1,\, \pm 3,\, ...,\, \pm\,(m-1)\}\,. \qquad (23)$$

We further consider uncoded and turbo-coded linear modulation. The turbo-coded transmission scheme encompasses the parallel concatenation of two identical binary 16-state rate-1/2 recursive systematic convolutional encoders with generator polynomials $(21)_8$ and $(37)_8$ in octal notation, via a pseudo random interleaver with block length N_b information bits, and an appropriate puncturing pattern so that the block at the turbo encoder output comprises N_c coded bits. This binary turbo code is followed by conventional Gray-mapped 2PAM or 4QAM modulation, giving rise to a block of N random data symbols, with $N = N_c = 3N_b$ for the case 2PAM and $N = N_c/2 = N_b$ for the case of 4QAM.

Our simulation results confirm that the high-SNR limit of the CRBs equals the MCRB. Comparing the CRBs for coded and uncoded transmission we observe that for a given constellation type they are equal at sufficiently high SNRs. At lower SNRs, however, there is a gap between the CRBs for coded and uncoded transmission. When E_s/N_0 decreases, a point $(E_s/N_0)_{thr}$ is reached where the CRBs start to diverge from their high-SNR limit. For coded transmission, $(E_s/N_0)_{thr}$ corresponds to a coded BER of about 10^{-3}. For uncoded transmission, $(E_s/N_0)_{thr}$ corresponds to an uncoded BER of about 10^{-3}, and consequently exceeds $(E_s/N_0)_{thr}$ for coded transmission by an amount equal to the coding gain.

For uncoded transmission the following observations can further be made:

- For both constellation types (PAM, QAM), we observe that for a given value of E_s/N_0 the CRB increases with M, which indicates that for the larger constellations carrier recovery is inherently harder to accomplish. This effect is clearly evident for MQAM, in which case the curves corresponding to large M exhibit an almost horizontal portion, but almost unnoticeable for MPAM. Fig. 3 also shows the limiting curve for M approaching infinity; this situation corresponds to data symbols that are continuous random variables, that are uniformly distributed in the interval $[-\sqrt{3}, \sqrt{3}]$ for PAM and in a square with side $\sqrt{6}$ for QAM. In the case of infinite-size constellations the CRBs do not necessarily converge to the corresponding MCRBs for large SNR; according to [11]. This is due to the non-diagonal nature of the FIM, related to the joint likelihood function $p\,(\mathbf{r}\,|\mathbf{a}, \mathbf{u}\,)$ of $\mathbf{a}$ and $\mathbf{u}$, with $\mathbf{u} = [\varphi_0, \varphi_1]$.
- For finite M, the CRB does converge to the MCRB when E_s/N_0 is sufficiently large. The value of E_s/N_0, at which CRB is close to MCRB, increases by about 6 dB when M doubles (PAM) or quadruples (QAM). This indicates that for uncoded pilot-symbol-free transmission, the convergence of the CRB to the MCRB is mainly determined by the value of $\frac{E_s}{N_0}\,(d_M)^2$, with d_M denoting the minimum Euclidean distance between the constellation points. Furthermore, at the normal operating SNR of uncoded digital communication systems, the CRBs turn out to be very well approximated by the corresponding MCRBs.

B. *Non-constant complex amplitude = Gaussian*

The multiplicative noise $a(n)$ is hereafter assumed to be a white non-circular Gaussian process with zero-mean, unit-variance, and pseudo-variance $c_a = \mathbb{E}[a(n)^2]$. For sake of simplicity, we also assume that the real part of $a(n)$ is independent of its imaginary part. This implies that c_a is real-valued. If $c_a = 0$, then $a(n)$ is circular; if $c_a = 1$, then $a(n)$ is real-valued. Thus, c_a quantifies the non-circularity rate of $a(n)$. We also set $\mathrm{SNR(in\ dB)} = 10\log_{10}(1/\sigma_w^2)$.

In each figure, we display four curves. Dashed lines correspond to the empirical MSEE for the well-known Square-Power (SP) estimate [1], [31], [34]. Solid lines with star-shape markers represent the ZZB. Solid lines with triangular-shaped markers represent the BB. Solid lines with circular-shaped markers represent the CRB. [31], [53]

In Fig. 4, we plot all the curves versus the SNR with $N = 64$, $c_a = 1$. We observe that the well-known outliers effect occurs at low and medium SNR [33]. We also observe that the ZZB is significantly tighter than the BB. The SNR threshold corresponding to the SP-based estimate is much larger than that one observed with the BB while the threshold value predicted by the ZZB is quite close to that obtained empirically with the SP estimate. As a consequence, the ZZB seems to be more powerful than the BB.

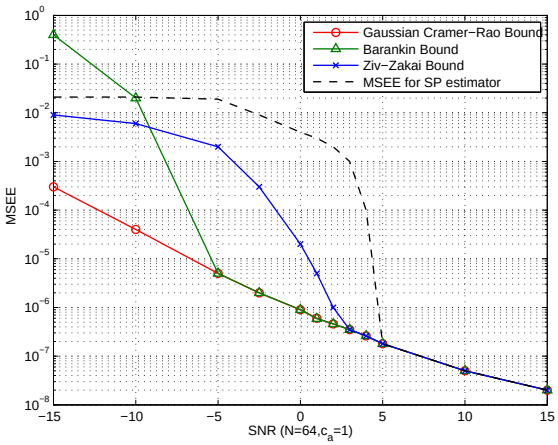

Figure 4. MSEE versus SNR

In Fig. 5, we plot the curves versus N with $\mathrm{SNR} = 10\mathrm{dB}$, $c_a = 0.9$. Even though the ZZB offers a more realistic value for the N threshold than the BB, the mismatch between the ZZB and the SP MSEE performance is still quite large.

In Fig. 6, the curves are displayed versus c_a with $N = 64$, $\mathrm{SNR} = 10\mathrm{dB}$. One can notice that the more $a(n)$ is non-circular (i.e., c_a increases), the better the estimation performance. Furthermore, the outliers effect rapidly degrades the performance if $a(n)$ is not non-circular enough. The figure confirms that accurate frequency estimation is really difficult to achieve when the white signal is not non-circular enough.

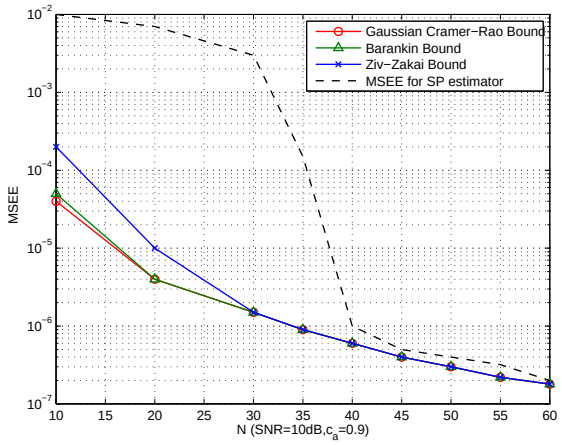

Figure 5. MSEE versus N

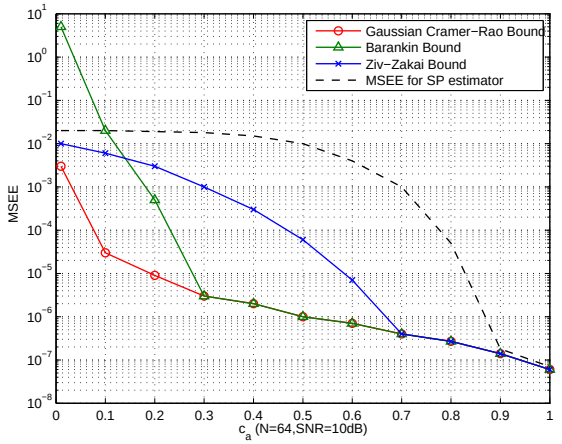

Figure 6. MSEE versus c_a

VIII. Conclusions

In this tutorial, we have focussed on the derivation and the analysis of fundamental lower bounds on the achievable MSEE for estimating the frequency and the phase of a received signal, when the complex amplitude of the signal is non-constant and unknown. In particular, the following application fields have been considered: digital communications, direction of arrival estimation, Doppler radar, etc... An overview of lower bounds (CRB, MCRB, BB and ZZB) with their respective interests and their associated derivations in closed-form for various cases has been presented.

References

[1] O. Besson and P. Stoica. "Nonlinear least-squares approach to frequency estimation and detection for sinusoidal signals with arbitrary envelope". *Digital Signal Processing*, 1:45–56, January 1999.

[2] M. Ghogho, A.K. Nandi, and A. Swami. "Cramer-Rao bounds and maximum likelihood estimation for random amplitude phase-modulated signals". *IEEE Trans. on Signal Processing*, 47:2905–2916, November 1999.

[3] M. Ghogho, A. Swami, and T.S. Durrani. "Frequency estimation in the presence of Doppler spread : performance analysis". *IEEE Trans. on Signal Processing*, 49:777–789, April 2001.

[4] H. Meyr, M. Moeneclaey and S.A. Fechtel. *Synchronization, channel estimation, and signal processing*, volume 2 of *Digital Communication Receivers*. John Wiley & Sons, 1997.

[5] C. Berrou, A. Glavieux and P. Thitimajsima. "Near Shannon limit error-correcting coding and decoding: turbo codes". In *Proc. IEEE International Conference on Communications (ICC)*, pages 1064–1070, Geneva, Switzerland, May 1993.

[6] R.G. Gallager. "Low density parity-check codes". *IRE Transactions on Information Theory*, 8:21–29, January 1962.

[7] D.J.C. MacKay. "Good error-correcting codes based on very sparse matrices". *IEEE Transactions on Information Theory*, 45(2):399–431, March 1999.

[8] G. Caire, G. Taricco and E. Biglieri. "Bit-interleaved coded modulation". *IEEE Transactions on Information Theory*, 44(3):927–946, May 1998.

[9] N.A. D'Andrea, U. Mengali and R. Reggiannini. "The Modified Cramer-Rao Bound and its Application to Synchronization Problems". *IEEE Transactions on Communications*, 42(2/3/4):1391–1399, March 1994.

[10] F. Gini, R. Reggiannini and U. Mengali. "The Modified Cramer-Rao Bound in Vector Parameter Estimation". *IEEE Transactions on Communications*, 46(1):52–60, January 1998.

[11] M. Moeneclaey. "On the true and the modified Cramer-Rao bounds for the estimation of a scalar parameter in the presence of nuisance parameters". *IEEE Transactions on Communications*, 46(11):1536–1544, November 1998.

[12] W.G. Cowley. "Phase and frequency estimation for PSK packets: bounds and algorithms". *IEEE Transactions on Communications*, 44(1):26–28, January 1996.

[13] F. Rice, B. Cowley, B. Moran and M. Rice. "Cramer-Rao lower bounds for QAM phase and frequency estimation". *IEEE Transactions on Communications*, 49(9):1582–1591, September 2001.

[14] H. Steendam and M. Moeneclaey. "Low-SNR limit of the Cramer-Rao bound for estimating the carrier phase and frequency of a PAM, PSK or QAM waveform". *IEEE Communications Letters*, 5(5):215–217, May 2001.

[15] N. Noels, H. Steendam and M. Moeneclaey. "The True Cramer-Rao bound for carrier frequency estimation from a PSK signal". *IEEE Transactions on Communications*, 52(5):834–844, May 2004.

[16] N. Noels, H. Steendam and M. Moeneclaey. "Carrier and clock recovery in (turbo) coded systems: Cramer-Rao bound and synchronizer performance". *EURASIP Journal on Applied Signal Processing*, pages 972–980, May 2005.

[17] N. Noels, H. Steendam, M. Moeneclaey and H. Bruneel. "Carrier phase and frequency estimation for pilot-symbol assisted transmission: bounds and algorithms". *IEEE Transactions on Signal Processing*, 53(12):4578–4587, December 2005.

[18] G.N. Tavares, L.M. Tavras and M.S.Piedade. "Improved Cramer-Rao Lower Bounds for Phase and Frequency Estimation with M-PSK Signals". *IEEE Transactions on Communications*, 49(12):2083–2087, December 2001.

[19] J.P. Delmas. "Closed-form expressions of the exact Cramer-Rao bound for parameter estimation of BPSK, MSK or QPSK waveforms". *IEEE Signal Processing Letters*, 15, April 2008.

[20] J. Ziv and M. Zakai. "Some Lower Bounds on Signal Parameter Estimation". *IEEE Transactions on Information Theory*, IT-15(3):386–391, May 1969.

[21] R.W. Miller and C.B. Chang. "A Modified Cramer-Rao Bound and its Applications". *IEEE Transactions on Information Theory*, IT-24(3):398–400, May 1978.

[22] F. Gini and R. Reggiannini. "On the use of Cramer-Rao-Like Bounds in the Presence of Random Nuisance Parameters". *IEEE Transactions on Communications*, 48(12):2120–2126, January 2000.

[23] J. Francos and B. Friedlander. "Bounds for estimation of multicomponent signals with random amplitude and deterministic phase". *IEEE Trans. on Signal Processing*, 43:1161–1172, May 1995.

[24] J. Francos and B. Friedlander. "Bounds for estimation of complex exponentials in unknown colored noise". *IEEE Trans. on Signal Processing*, 43:2176–2185, September 1995.

[25] G. Zhou and G.B. Giannakis. "Harmonics in gaussian multiplicative and additive white noise : Cramer-Rao bounds". *IEEE Trans. on Signal Processing*, 43:1217–1231, May 1996.

[26] G. Vazquez. *Signal Processing Advances for Wireless Mobile Comnuncations*, chapter 9 (Non-Data-Aided Digital Synchronization). Englewood Cliffs, Prentice-Hall, 2000.

[27] E.W. Barankin. "Locally best unbiaised estimates". *Annals of Mathematical Statistics*, 20:447–501, 1949.

[28] H. Messer. "Source localization performance and the array beampattern". *Signal Processing*, 28:163–181, August 1992.

[29] L. Knockaert. "The Barankin bound and threshold behavior in frequency estimation". *IEEE Trans. on Signal Processing*, 45:2398–2401, September 1997.

[30] A. Renaux, P. Forster, P. Larzabal, C. Richmond, and Arye Nehorai. "A fresh look at the bayesian bounds of the Weiss-Weinstein family". *IEEE Trans. on Signal Processing*, 56:5334–5352, November 2008.

[31] P. Ciblat, M. Ghogho, P. Larzabal, and P. Forster . "Harmonic retrieval in the presence of non-circular Gaussian multiplicative noise : Performance bounds". *Signal Processing*, 85:737–749, April 2005.

[32] H.L. Van Trees. *Detection, estimation, and modulation theory, Part I*. John Wiley & Sons, 2001.

[33] D.C. Rife and R.R. Boorstyn. "Single-tone parameter estimation from discrete-time observations". *IEEE Trans. on Information Theory*, 20:591–598, September 1974.

[34] M. Ghogho, A. Swami, and A.K. Nandi. Non linear least squares estimation for harmonics in multiplicative and additive noise. *Signal Processing*, 78:43–60, 1999.

[35] A. Hansson, K.M. Chugg and T.M. Aulin. "On forward-adaptive versus Forward/Backward-adaptive SISO algorithms for Rayleigh fading channels". *IEEE Communications Letters*, 5:477–479, December 2001.

[36] N. Noels. "Synchronization in Digital Communication Systems: Performance Bounds and Practical Algorithms". *Phd. dissertation, Faculty of Engineering, Ghent University*, 2009.
Available at http://telin.ugent.be/∼nnoels.

[37] N. Noels and M. Moeneclaey. "True Cramer-Rao bound for estimating synchronization parameters from a linearly modulated bandpass signal with unknow data symbols". In *Proc. 2nd IEEE International Workshop on Computational Advances in Multi-Sensor Adaptive Processing (CAMSAP)*, Saint Thomas, VI USA, December 2007.

[38] H.-A. Loeliger. "An introduction to factor graphs". *IEEE Signal Processing Magazine*, 21(1):28–41, January 2004.

[39] B. Picinbono. "On circularity". *IEEE Trans. on Signal Processing*, 42:3473–3482, December 1994.

[40] B. Porat. *Digital Signal Processing of Random Signals*. Prentice Hall, 1994.

[41] P. Whittle. "The analysis of multiple stationary time-series". *Journal of Royal Statistics Society*, 15:125–139, 1953.

[42] W. Jakes. *Microwave Mobile Communications*. John Wiley & Sons, 1975.

[43] R. Clarke. "A statistical theory of mobile radio reception". *Bell Systems Technical Journal*, 47:957–1000, June 1968.

[44] R.M. Gray. *Toeplitz and circulant matrices : a review*. Stanford EE Lab. Report, 2002.

[45] U. Grenander and G. Szegö. *Toeplitz forms and their applications*. Univ. California (Berkeley) Press, 1958.

[46] E.J. Hannan. The estimation of frequency. *Journal of Applied Probability*, 10:510–519, 1973.

[47] A.J. Viterbi and A.M. Viterbi. Non-linear estimation of PSK-modulated carrier phase with application to burst digital transmissions. *IEEE Trans. on Information Theory*, 29:543–551, July 1983.

[48] Y. Wang, E. Serpedin and P. Ciblat. Optimal blind nonlinear least-squares carrier phase and frequency offset estimation for general QAM modulations. *IEEE Trans. on Wireless Communications*, 2:1040–1054, September 2003.

[49] S.K. Chow and P.M. Schultheiss. "Delay estimation using narrow-band processes". *IEEE Trans. on Acoustics, Speech, and Signal Processing*, 29:478–484, June 1981.

[50] K.L. Bell, Y. Steinberg, Y. Ephraim, and H.L. Van Trees. "Extended Ziv-Zakai lower bound for vector parameter estimation". *IEEE Trans. on Information Theory*, 43:624–637, March 1997.

[51] Q. Zhang and D. Liu. A simple capacity formula for correlated diversity Rician fading channels. *IEEE Communications Letters*, 6(11):481–483, November 2002.

[52] M.K. Simon and M.S. Alouini. On the distribution of two Chi-square variates with application to outage probability computation. *IEEE Trans. on Communications*, 49(11):1946–1954, November 2001.

[53] P. Ciblat and M. Ghogho. "Ziv-Zakai bound for harmonic retrieval in multiplicative and additive Gaussian noise". In *Proc. IEEE Statistical Signal Processing Workshop (SSP)*, Bordeaux, France, July 2005.